PNAS RESEARCH ARTICLE | IMMUNOLOGY AND INFLAMMATION

Cross-talk between IL-6 trans-signaling and AIM2 inflammasome/IL-1β axes bridge innate immunity and epithelial apoptosis to promote emphysema

Saleela M. Ruwanpura[a,b], Louise McLeod[a,b], Lovisa F. Dousha[c], Huei J. Seow[c], Alison C. West[a,b], Alice J. West[a,b], Teresa Weng[a,b], Mohammad Alanazi[a,b], Martin MacDonald[d], Paul T. King[d], Philip G. Bardin[a,b,d], Cem Gabay[e,f], Dennis M. Klinman[g], Steven Bozinovski[h], Ross Vlahos[h], Gary P. Anderson[c], Stefan Rose-John[i], Mohamed I. Saad[a,b], and Brendan J. Jenkins[a,b,1]

Edited by Katherine Fitzgerald, University of Massachusetts Medical School, Worcester, MA; received January 28, 2022; accepted August 5, 2022

Pulmonary emphysema is associated with dysregulated innate immune responses that promote chronic pulmonary inflammation and alveolar apoptosis, culminating in lung destruction. However, the molecular regulators of innate immunity that promote emphysema are ill-defined. Here, we investigated whether innate immune inflammasome complexes, comprising the adaptor ASC, Caspase-1 and specific pattern recognition receptors (PRRs), promote the pathogenesis of emphysema. In the lungs of emphysematous patients, as well as spontaneous *gp130*$^{F/F}$ and cigarette smoke (CS)-induced mouse models of emphysema, the expression (messenger RNA and protein) and activation of ASC, Caspase-1, and the inflammasome-associated PRR and DNA sensor AIM2 were up-regulated. AIM2 up-regulation in emphysema coincided with the biased production of the mature downstream inflammasome effector cytokine IL-1β but not IL-18. These observations were supported by the genetic blockade of ASC, AIM2, and the IL-1 receptor and therapy with AIM2 antagonistic suppressor oligonucleotides, which ameliorated emphysema in *gp130*$^{F/F}$ mice by preventing elevated alveolar cell apoptosis. The functional requirement for AIM2 in driving apoptosis in the lung epithelium was independent of its expression in hematopoietic-derived immune cells and the recruitment of infiltrating immune cells in the lung. Genetic and inhibitor-based blockade of AIM2 also protected CS-exposed mice from pulmonary alveolar cell apoptosis. Intriguingly, IL-6 trans-signaling via the soluble IL-6 receptor, facilitated by elevated levels of IL-6, acted upstream of the AIM2 inflammasome to augment AIM2 expression in emphysema. Collectively, we reveal cross-talk between the AIM2 inflammasome/IL-1β and IL-6 trans-signaling axes for potential exploitation as a therapeutic strategy for emphysema.

AIM2 | emphysema | inflammasome | apoptosis | IL-6

Significance

Chronic lung inflammation triggered by dysregulated activation of innate immunity is implicated in pulmonary emphysema. However, key innate immune molecular regulators that trigger emphysema remain ill-defined. We reveal innate immune multiprotein inflammasome complexes comprising the AIM2 cytosolic DNA sensor as key drivers of pulmonary emphysema. The requirement for AIM2 was independent of inflammation but rather via a direct effect of the AIM2 inflammasome in augmenting alveolar epithelial apoptosis. Furthermore, we discover that AIM2 is upregulated in emphysema by cross-talk with the immunomodulatory cytokine interleukin 6. These findings lay the foundation for the future design and clinical application of novel innate immune-based therapeutics against emphysema.

Emphysema is a major debilitating component of chronic obstructive pulmonary disease (COPD), the third leading cause of morbidity and mortality worldwide (1, 2). The main cause of emphysema is cigarette smoke (CS), which triggers potent innate immune responses leading to chronic pulmonary inflammation that damages lung structure and health in most smokers, ∼20% of whom develop clinically debilitating, irreversible emphysema (3, 4). Pulmonary inflammation is characterized by increased expression of many proinflammatory cytokines, including interleukin (IL)-6, which is also a common feature of emphysema patients and has been linked to disease pathogenesis in several preclinical emphysema models (5–10). These include *gp130*$^{F/F}$ mice, which are genetically engineered for IL-6/gp130–dependent hyperactivation of "trans" signaling—the pathological mode of signaling by IL-6 upon its engagement with the naturally occurring soluble IL-6 receptor (sIL-6R)—which in the lung drives alveolar cell apoptosis, leading to emphysema (7, 11). However, the identity of key regulators of innate immunity which contribute to emphysema susceptibility and progression remain ill-defined.

Innate immune responses to microbes and endogenous host-derived danger (or damage) signals within the lung mucosa depend on the tightly coordinated activation of extracellular and cytosolic pattern recognition receptors (PRRs), which are widely expressed in epithelial and immune cells. PRRs are classified into several large structurally and functionally conserved families, including toll-like receptors (TLRs), absent in melanoma 2 (AIM2)-like receptors (ALRs), and NOD-like receptors (NLRs) (3, 12, 13). The activation of specific ALRs and NLRs initiates inflammatory signaling cascades via multiprotein complexes called inflammasomes, which comprise the key adaptor protein apoptosis-associated speck-like protein containing a caspase recruitment domain (ASC), and Caspase-1, to facilitate maturation and release of proinflammatory cytokines IL-1β and IL-18 (3, 13, 14). Although inflammasomes are critical for driving acute innate

Author contributions: B.J.J. designed research; S.M.R., L.M., L.F.D., H.J.S., A.C.W., A.J.W., T.W., M.A., S.B., R.V., and M.I.S. performed research; M.M., P.T.K., P.G.B., C.G., D.M.K., G.P.A., and S.R.-J. contributed new reagents/analytic tools; S.M.R., L.M., R.V., M.I.S., and B.J.J. analyzed data; and B.J.J. wrote the paper.

The authors declare no competing interest.

This article is a PNAS Direct Submission.

[1]To whom correspondence may be addressed. Email: Brendan.Jenkins@hudson.org.au.

This article contains supporting information online at http://www.pnas.org/lookup/suppl/doi:10.1073/pnas.2201494119/-/DCSupplemental.

Published August 29, 2022.

immune responses that resolve inflammation and maintain tissue homeostasis, data from clinical studies and mouse disease models demonstrate that excessive inflammasome activation promotes several chronic autoimmune and inflammatory diseases (3, 13, 15).

The potential involvement of inflammasomes in COPD has been suggested from observations that CS induces Caspase-1 activity, and IL-1β and IL-18 production, in vitro (lung epithelial cells) and in vivo (16–20). Also, experimentally induced (i.e., CS, elastase, or ozone) COPD mouse models either involving mice lacking receptors for IL-1β and IL-18 or treated with an IL-1 receptor antagonist or a Caspase-1 inhibitor are protected against airway inflammation (17–19, 21, 22). Clinical studies have also shown increased Caspase-1 activity, and elevated IL-1β and IL-18 levels, in lungs of COPD patients and smokers (16, 18, 20, 23). Moreover, the extracellular release of ASC specks, another indicator of inflammasome activity, has been reported in bronchoalveolar lavage fluid (BALF) of COPD patients and a CS-induced COPD mouse model (24). However, the role of specific inflammasome-associated PRRs in emphysema is unknown, with investigations limited to the observation that *Nlrp3*$^{-/-}$ mice are protected against a CS-induced COPD-like phenotype in the lung, although emphysema-specific criteria were not reported (25).

To address this knowledge gap in the role of inflammasomes in the pathogenesis of emphysema, here we show that components of AIM2 inflammasomes, namely ASC, Caspase-1, and AIM2, were overexpressed and/or hyperactivated in lungs of genetically engineered spontaneous *gp130*$^{F/F}$ and acute CS-induced emphysema mouse models and in lungs of emphysema patients. Genetic ablation of ASC and AIM2, but not NLRP3, in these preclinical models ameliorated emphysematous changes by suppressing elevated alveolar cell apoptosis, independent of infiltrating immune cells, in the lung epithelium. Furthermore, we show that the AIM2 inflammasome preferentially employs IL-1β, but not IL-18, to drive emphysema. We also reveal that IL-6 trans-signaling was an upstream regulator of AIM2 expression and inflammasome activation in emphysema. Collectively, our findings provide critical evidence to consider the innate immune AIM2 inflammasome/IL-1β axis as a potential new treatment strategy for emphysematous COPD patients.

Methods

Human Samples. Lung tissue from surgery for treatment of a solitary peripheral carcinoma was collected at Monash Medical Centre (Melbourne, Australia) from patients with or without evidence of emphysema, defined by pulmonary function tests (7) (*SI Appendix*, Table S1) and high-resolution computerized tomography of the chest. Tissues from tumor-free subpleural parenchyma were formalin-fixed and paraffin-embedded or snap-frozen. Lung tissue and sera (including from healthy emphysema-free individuals) were collected upon written informed consent. Studies were approved by the Monash Health Human Research Ethics Committee.

Animal Models and Treatments. The *gp130*$^{F/F}$, *gp130*$^{F/F}$:*Aim2*$^{-/-}$, *gp130*$^{F/F}$:*Asc*$^{-/-}$, *gp130*$^{F/F}$:*Il1r*$^{-/-}$, *gp130*$^{F/F}$:*Il18*$^{-/-}$, *gp130*$^{F/F}$:*sgp130Fc*$^{tg/tg}$, and *gp130*$^{F/F}$:*Il6*$^{-/-}$ mice and *Aim2*$^{-/-}$, *Nlrp3*$^{-/-}$, and *sgp130Fc*$^{tg/tg}$ mice, on a 129Sv × C57BL/6 background, have been reported (7, 8, 26–28). Experiments involving *gp130*$^{F/F}$ mice treated with the AIM2 antagonist Sup ODN or the IL-6 trans-signaling inhibitor sgp130Fc have been described (7, 26). The acute CS model was performed on wild-type (WT), *Aim2*$^{-/-}$, and *sgp130Fc*$^{tg/tg}$ mice as before (7, 8), with WT mice also concurrently administered by intraperitoneal injection with sgp130Fc (once, 0.5 mg/kg), rapamycin (twice, 4 mg/kg) or Sup ODN (once, 15 mg/kg), along with relative control injections, over 4 d. Bone marrow chimeras were generated as before (26).

All mice were housed under specific pathogen-free conditions. Experiments were approved by the Monash University Animal Ethics Monash Medical Centre "B" Committee and were conducted in accordance with the ARRIVE guidelines (29).

Lung Function Analyses and Assessment of Emphysema. Histological assessment of perfusion-fixed mouse lungs was performed on methylene blue-stained lung tissue sections using computer-assisted newCAST software (version 2.14; Visiopharm), and airspace enlargement was quantified by mean linear intercept (MLI) on hematoxylin and eosin (H&E)-stained lung sections (7, 8). Lung function was performed using the flexiVent system (SCIREQ) (7, 8).

Immunofluorescence and Immunohistochemistry. Formalin-fixed, paraffin-embedded human lung sections were stained with antibodies against AIM2 (HPA031365; Atlas Antibodies) and cleaved Caspase-1 (PA5-38099; Invitrogen) (26). Terminal deoxynucleotidyl transferase-mediated dUDP nick-end labeling (TUNEL) assay (Millipore) and immunohistochemistry with antibodies against AIM2 (20590-1-AP; Proteintech), CD45 (ab40763; Abcam), ASC (AL177; Adipogen), and cleaved (Asp210) Caspase-1 (PA5-38099; Invitrogen) were performed on mouse lung tissue sections (7, 26). Positive-staining cells were quantified manually on digital images of photomicrographs (60× high-power fields; $n = 20$ per lung section) (7).

Multicolor immunofluorescence staining was performed on paraffin-embedded lung tissues using antibodies against cleaved Caspase-3/Alexa Fluor 488 (9669; Cell Signaling Technology) or ASC (AG-25B-006; Adipogen), AIM2 (20590-1-AP; Proteintech), gamma-H2AX (ab2893, phospho S139; Abcam), SPC (SC-7706; Santa Cruz Biotechnology), and CD45 (ab40763; Abcam) together with Alexa Fluor 568-conjugated donkey anti-goat and Alexa Fluor 488-conjugated donkey anti-rabbit secondary antibodies (Abcam) (7, 26, 30). Nuclear staining was achieved using 4′,6-diamidino-2-phenylindole (DAPI). Slides were examined under a Nikon confocal microscope and analyzed for red and green fluorescence. Where appropriate, stereological techniques were applied to determine dual-stained cell numbers (7). To assess for the presence of ASC specks within SPC-positive cells, z-stack confocal imaging was performed by capturing 16 to 18 z-stacks of 0.5-μm size at 100× magnification.

ELISA and Immunoblotting. Total protein lysates were prepared from snap-frozen lung tissues (27) and with sera were subjected to enzyme-linked immunosorbent assay (ELISA) and/or immunoblotting. ELISA was performed for mouse and human total IL-1β and sIL-6R (R&D Systems), mouse/human IL-6 (BD Sciences), and mouse/human total IL-18 (MBL International Corporation). Mature/free human IL-18 was detected with a sandwich ELISA (27). Immunoblotting was performed with antibodies against mouse cleaved Caspase-1 (AG-20B-0042-C100; AdipoGen), IL-18 (5180R; BioVision), IL-1β (AF-401-NA; R&D Systems), AIM2 (20590-1-AP; Proteintech), cleaved Caspase-3 (9661; Cell Signaling Technology), Gasdermin D (ab209845; Abcam), and β-tubulin (ab6046; Abcam). Protein bands were visualized using enhanced chemiluminescence for Caspase-1 or for other immunoblots with the Odyssey Infrared Imaging System (LI-COR) and quantified using ImageJ (NIH).

RNA Isolation and Gene Expression Analyses. Total RNA was isolated from snap-frozen mouse and human lung tissues using TRIzol (Sigma), and quantitative RT-PCR (qPCR) was performed on complementary DNA (triplicates) with SYBR Green (Life Technologies) using the 7900HT Fast RT-PCR System (Applied Biosystems). Gene expression data were analyzed using the Sequence Detection System Version 2.4 software (Applied Biosystems). Mouse and human primer sequences have been described previously (8, 26, 27, 30).

Statistical Analyses. Statistics were performed using GraphPad Prism for Windows version 7.0 software, with D'Agostino and Pearson omnibus K2 normality tests. Significance between two groups of normal distribution was determined by Student's *t* tests, and Mann–Whitney *U* tests were performed for nonnormally distributed data or smaller data sets. One-way ANOVA was used to determine differences among three or more groups for normally distributed data, and Kruskal–Wallis tests for nonnormally distributed data or smaller datasets. Linear regression was performed for correlations between given markers in emphysema patient groups only. A P value of <0.05 was considered statistically significant. Experimental sample size estimates were based on power analyses assuming a significance level (alpha) of 0.05 and a power of 80%. All data in figures are expressed as the mean ± SEM.

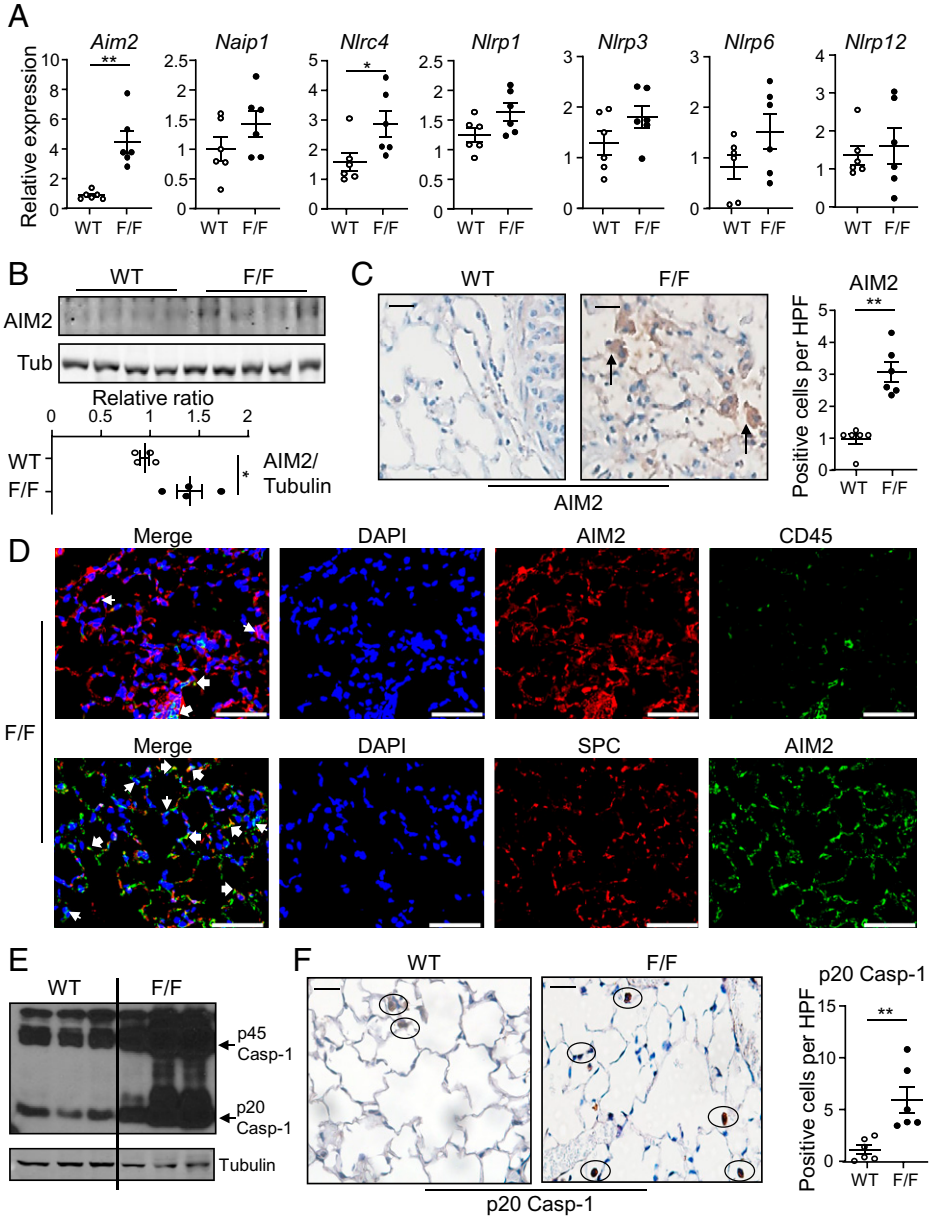

Fig. 1. Augmented expression and activation of AIM2 inflammasome components in lungs of emphysematous *gp130*$^{F/F}$ mice. (*A*) qPCR on lung tissue of 6mo WT and *gp130*$^{F/F}$ (F/F) mice. Expression data normalized for 18S ribosomal RNA (rRNA). $n = 6$ per genotype. $^{*}P < 0.05$, $^{**}P < 0.01$; Student's *t* test. (*B*) Representative AIM2 immunoblots on lung lysates from 6mo WT and F/F mice. Also shown is densitometric quantification of the immunoblot for AIM2 protein levels, normalized against tubulin. $n = 4$ per genotype. $^{*}P < 0.05$; Student's *t* test. (*C*) Representative photomicrographs of cross-sections of lungs from 6mo WT and F/F mice stained with an anti-AIM2 antibody. Graph depicts quantification of AIM2-positive cell numbers. $n = 6$ per genotype. $^{**}P < 0.01$; Student's *t* test. (Scale bars, 20 μm.) (*D*) Representative immunofluorescence photomicrographs of cells positive for either CD45 (green, *Top*), SPC (red, *Bottom*), AIM2 (red, *Top*; green, *Bottom*), or both AIM2 and CD45 (yellow and/or white, *Top*, merged) or AIM2 and SPC (yellow and/or white, *Bottom*, merged), in lung cross-sections of a 6mo F/F mouse. DAPI nuclear staining is blue. In merged images, white block arrows point to representative colocalized staining of AIM2 and CD45 (*Top*) or AIM2 and SPC (*Bottom*), and white arrowheads point at representative AIM2 nuclear staining. (Scale bars, 50 μm.) (*E*) Representative immunoblots on lung lysates from 6mo WT and F/F mice for pro (45 kDa) and cleaved (20 kDa) Caspase-1. (*F*) Representative photomicrographs of cross-sections of lungs from 6mo WT and F/F mice stained with an anti-cleaved (p20) Caspase-1 antibody. Representative positively stained cells are circled. Graph depicts quantification of cleaved Caspase-1–positive cell numbers per high-power field (HPF). (Scale bars, 20 μm.) $n = 6$ per genotype. $^{**}P < 0.01$; Student's *t* test.

Results

Augmented Expression and Activation of Inflammasome Components Correlates with the Emphysema Phenotype of the *gp130*$^{F/F}$ Mouse Model. We initially profiled the gene expression of inflammasome-associated PRRs in emphysematous lungs of 6-month-old (mo) *gp130*$^{F/F}$ mice by qPCR. Messenger RNA (mRNA) expression of *Aim2* (4.5-fold) and *Nlrc4* (2-fold) was significantly up-regulated in lungs of *gp130*$^{F/F}$ mice versus control *gp130*$^{+/+}$ mice, while *Nlrp3*, *Nlrp1*, *Naip1*, *Nlrp6*, and *Nlrp12* remained unchanged (Fig. 1*A*). *Aim2* was the most highly expressed inflammasome-associated PRR gene in emphysematous *gp130*$^{F/F}$ mouse lungs (*SI Appendix*, Fig. S1). Considering the high mRNA levels of *Aim2*, we next evaluated AIM2 protein expression by immunoblotting and immunohistochemistry. Indeed, AIM2 protein expression levels, and AIM2-positive cell numbers, were also significantly increased in the lungs of 6mo *gp130*$^{F/F}$ mice, with immunohistochemistry revealing a staining pattern in the parenchyma indicative of predominant expression in alveolar type II (ATII) epithelial cells (Fig. 1 *B* and *C*). Immunofluorescence further supported the pronounced colocalization of AIM2 with SPC-positive ATII cells, and to a lesser extent CD45-positive immune cells, with AIM2 detected in both nuclear and cytoplasmic cellular compartments (Fig. 1*D* and *SI Appendix*, Fig. S2*A*).

Next, we assessed the expression and/or activation status of inflammasome components ASC (encoded by the *Pycard* gene) and Caspase-1 (*Casp1*) in the lungs of emphysematous 6mo *gp130*$^{F/F}$ mice. qPCR analyses indicated that both *Pycard* and *Casp1* mRNA levels were significantly elevated in *gp130*$^{F/F}$ emphysematous lungs compared to lungs from emphysema-free control WT mice (*SI Appendix*, Fig. S2*B*). Immunoblotting also demonstrated significantly elevated protein expression of pro (45 kDa) and mature/active (20 kDa) Caspase-1 in *gp130*$^{F/F}$ emphysematous lungs (Fig. 1*E* and *SI Appendix*, Fig. S2*C*). Immunohistochemistry also showed significant increases in numbers of ASC-positive and active Caspase-1–positive cells, predominantly ATII cells by their distinct morphology and immunofluorescence colocalization (for ASC) with SPC-positive ATII epithelial cells, in the lung parenchyma of *gp130*$^{F/F}$ mice versus WT controls (Fig. 1*F* and *SI Appendix*, Fig. S2 *D*–*G*).

These data indicate heightened expression and/or activation of ASC-containing inflammasome components (i.e., ASC, Caspase-1, and AIM2) mainly in the lung epithelium during emphysema in the *gp130*$^{F/F}$ model.

Emphysema in *gp130*$^{F/F}$ Mice Is Driven by the AIM2, but Not NLRP3, Inflammasome. We next evaluated whether elevated AIM2 expression promotes emphysema in *gp130*$^{F/F}$ mice by crossing *gp130*$^{F/F}$ mice with *Aim2*$^{-/-}$ mice. Histological evaluation of 6mo *gp130*$^{F/F}$:*Aim2*$^{-/-}$ mice revealed normal alveolar lung architecture compared to enlargement of the distal air spaces and destruction of alveoli, measured as alveolar MLI, that are a feature of emphysematous *gp130*$^{F/F}$ mice (Fig. 2 *A* and *B*). Consistent with these histological observations, elevated static compliance and lung volume in *gp130*$^{F/F}$ mice, due to destruction of elastic fibers in emphysematous lungs (8), were reduced to normal in *gp130*$^{F/F}$:*Aim2*$^{-/-}$ mice (Fig. 2 *C* and *D*). Also, protein expression of pro and active Caspase-1 was significantly reduced in 6mo *gp130*$^{F/F}$:*Aim2*$^{-/-}$ versus *gp130*$^{F/F}$ mice (Fig. 2 *E* and *F*). By contrast, in NLRP3-deficient *gp130*$^{F/F}$:*Nlrp3*$^{-/-}$ mouse lungs these emphysema features of *gp130*$^{F/F}$ mice were similarly observed, and pro and active Caspase-1 levels were not reduced but rather remained elevated (Fig. 2 *A–D* and *SI Appendix*, Fig. S3 *A* and *B*).

We next evaluated whether AIM2-driven emphysema was dependent upon inflammasome activity by generating *gp130*$^{F/F}$ mice deficient for the key inflammasome adaptor, ASC (*gp130*$^{F/F}$:*Asc*$^{-/-}$). Indeed, 6mo *gp130*$^{F/F}$:*Asc*$^{-/-}$ mice displayed an alveolar lung architecture comparable to WT mice (Fig. 2*G*). Similarly, compared to *gp130*$^{F/F}$ mice, MLI, static compliance, and lung volume were significantly reduced to normal levels in *gp130*$^{F/F}$:*Asc*$^{-/-}$ mice (Fig. 2 *H–J*). Consistent with a critical role for ASC in inflammasome activity, protein expression levels of pro and active Caspase-1 were significantly reduced in 6mo *gp130*$^{F/F}$:*Asc*$^{-/-}$ versus *gp130*$^{F/F}$ mice (*SI Appendix*, Fig. S3 *C* and *D*). Collectively, these data suggest that AIM2 is the predominant PRR in the lung that contributes to inflammasome activation and the development of emphysema in *gp130*$^{F/F}$ mice.

Increased Production of IL-1β, but Not IL-18, Is Associated with AIM2 Inflammasome-Mediated Emphysema in *gp130*$^{F/F}$ Mice. To elucidate a role for the AIM2 inflammasome effector cytokines IL-1β and/or IL-18 in emphysema pathogenesis, we initially measured IL-1β and IL-18 expression levels in the lungs of 6mo *gp130*$^{F/F}$ mice. At the mRNA (qPCR) and protein (ELISA) levels, expression of IL-1β and IL-18 were significantly increased in lung tissues of *gp130*$^{F/F}$ mice compared to normal lung tissue of WT mice, with ELISA indicating a 20- to 30-fold increase in total (pro and mature) protein levels of IL-1β compared to IL-18 in lung tissues (Fig. 3 *A* and *B*). Interestingly, immunoblotting revealed that both pro (31 kDa) and mature (17 kDa) IL-1β were significantly up-regulated in *gp130*$^{F/F}$ emphysematous lungs versus WT lungs, whereas only pro (24 kDa) IL-18 protein levels (elevated) were detected in lung lysates of *gp130*$^{F/F}$ versus WT mice (Fig. 3 *C–F*). Furthermore, immunoblotting and/or ELISA showed that mature and/or total IL-1β protein levels were reduced in lungs of both 6mo emphysema-free *gp130*$^{F/F}$:*Aim2*$^{-/-}$ and *gp130*$^{F/F}$:*Asc*$^{-/-}$ mice versus emphysematous *gp130*$^{F/F}$ mice, consistent with a disease association for IL-1β in AIM2 inflammasome-driven emphysema (Fig. 3 *G–I*).

Since these findings suggested an increase in the inflammasome-mediated production of mature IL-1β, but not IL-18, during emphysema in *gp130*$^{F/F}$ mice, we next assessed whether IL-1β preferentially promoted emphysema pathogenesis by crossing *gp130*$^{F/F}$ mice with mice lacking either the IL-1 receptor (*gp130*$^{F/F}$:*Il1r*$^{-/-}$) or IL-18 (*gp130*$^{F/F}$:*Il18*$^{-/-}$). Histological evaluation of 6mo *gp130*$^{F/F}$:*Il1r*$^{-/-}$ mice revealed normal alveolar lung architecture compared to enlargement of the distal air spaces and destruction of alveoli in the lungs of *gp130*$^{F/F}$ mice (Fig. 3*J*). Also, static compliance and lung volume were significantly reduced in 6mo *gp130*$^{F/F}$:*Il1r*$^{-/-}$ versus *gp130*$^{F/F}$ mice (Fig. 3 *K* and *L*). By contrast, lung histology, static compliance, and lung volume remained comparable between 6mo *gp130*$^{F/F}$ and *gp130*$^{F/F}$:*Il18*$^{-/-}$ mice (Fig. 3 *J–L*). Taken together, these findings suggest that AIM2 inflammasome-associated emphysematous changes in the lungs of *gp130*$^{F/F}$ mice are driven via the preferential processing of IL-1β.

Inflammasome-Driven Emphysema in *gp130*$^{F/F}$ Mice Is Characterized by Augmented Cell Apoptosis, Independent of Infiltrating Immune Cells in the Lung. We next investigated whether suppressed emphysema in *gp130*$^{F/F}$:*Aim2*$^{-/-}$, *gp130*$^{F/F}$:*Asc*$^{-/-}$, and *gp130*$^{F/F}$:*Il1r*$^{-/-}$ mice is associated with diminished lung inflammation. Histologic assessment of H&E-stained lung tissue sections from 6mo mice revealed that the elevated pulmonary inflammation score (compared to WT mice) was comparable among *gp130*$^{F/F}$, *gp130*$^{F/F}$:*Aim2*$^{-/-}$, *gp130*$^{F/F}$:*Asc*$^{-/-}$, and *gp130*$^{F/F}$:*Il1r*$^{-/-}$ mice (*SI Appendix*, Fig. S4*A*). Immunohistochemical analyses also indicated comparable numbers of infiltrating CD45-positive leukocytes in lungs of these *gp130*$^{F/F}$-based mouse strains (*SI Appendix*, Fig. S4*B*). Also, mRNA expression of inflammatory genes *Il6*, *Cxcl2*, *Ifng*, and *Tnfa* were comparable between genotypes, which for IL-6 protein expression was also confirmed by ELISA (*SI Appendix*, Fig. S4 *C* and *D*).

The unaltered pulmonary immune cell infiltrates in *gp130*$^{F/F}$:*Aim2*$^{-/-}$ mice, together with the specific up-regulation of AIM2 in the lung epithelium, suggested that AIM2-expressing immune cells do not play a major role in the pathogenesis of emphysema. In support of this notion, bone marrow chimeras generated by reconstitution of irradiated *gp130*$^{F/F}$ recipients with bone marrow from *gp130*$^{F/F}$ or *gp130*$^{F/F}$:*Aim2*$^{-/-}$ donor mice revealed that irrespective of the genotype of the donor bone marrow there was no effect on the onset of pulmonary emphysema (or infiltration of immune cells) in *gp130*$^{F/F}$ recipients (*SI Appendix*, Fig. S5 *A–D*). Collectively, these data suggest that *Aim2* expression in the nonhematopoietic compartment (i.e., epithelium) promotes emphysema.

Since emphysema in *gp130*$^{F/F}$ mice is associated with a high apoptosis index of ATII cells (8), we next investigated whether the AIM2/ASC/IL-1β axis contributed to increased apoptosis of the alveolar epithelium. TUNEL-positive apoptotic cell numbers were significantly reduced in 6mo emphysema-free *gp130*$^{F/F}$:*Aim2*$^{-/-}$, *gp130*$^{F/F}$:*Asc*$^{-/-}$ and *gp130*$^{F/F}$:*Il1r*$^{-/-}$ mice versus emphysematous *gp130*$^{F/F}$ mice (Fig. 4 *A* and *B*). Immunofluorescence for cleaved Caspase-3 (apoptosis) and SPC (ATII cells) confirmed a significant decrease in the number of apoptotic SPC-positive ATII cells in lungs of WT, *gp130*$^{F/F}$:*Aim2*$^{-/-}$, *gp130*$^{F/F}$:*Asc*$^{-/-}$, and *gp130*$^{F/F}$:*Il1r*$^{-/-}$ mice versus *gp130*$^{F/F}$ mice (Fig. 4*C* and *SI Appendix*, Fig. S6*A*). These observations were also supported by immunoblotting, which indicated elevated protein expression levels of fully mature/cleaved (p17) Caspase-3 in lung lysates of 6mo *gp130*$^{F/F}$ mice compared to either WT or *gp130*$^{F/F}$:*Aim2*$^{-/-}$ mice (*SI Appendix*, Fig. S6*B*). We also observed that, consistent with gasdermin D (GSDMD) not being required for Caspase-1 (i.e.,

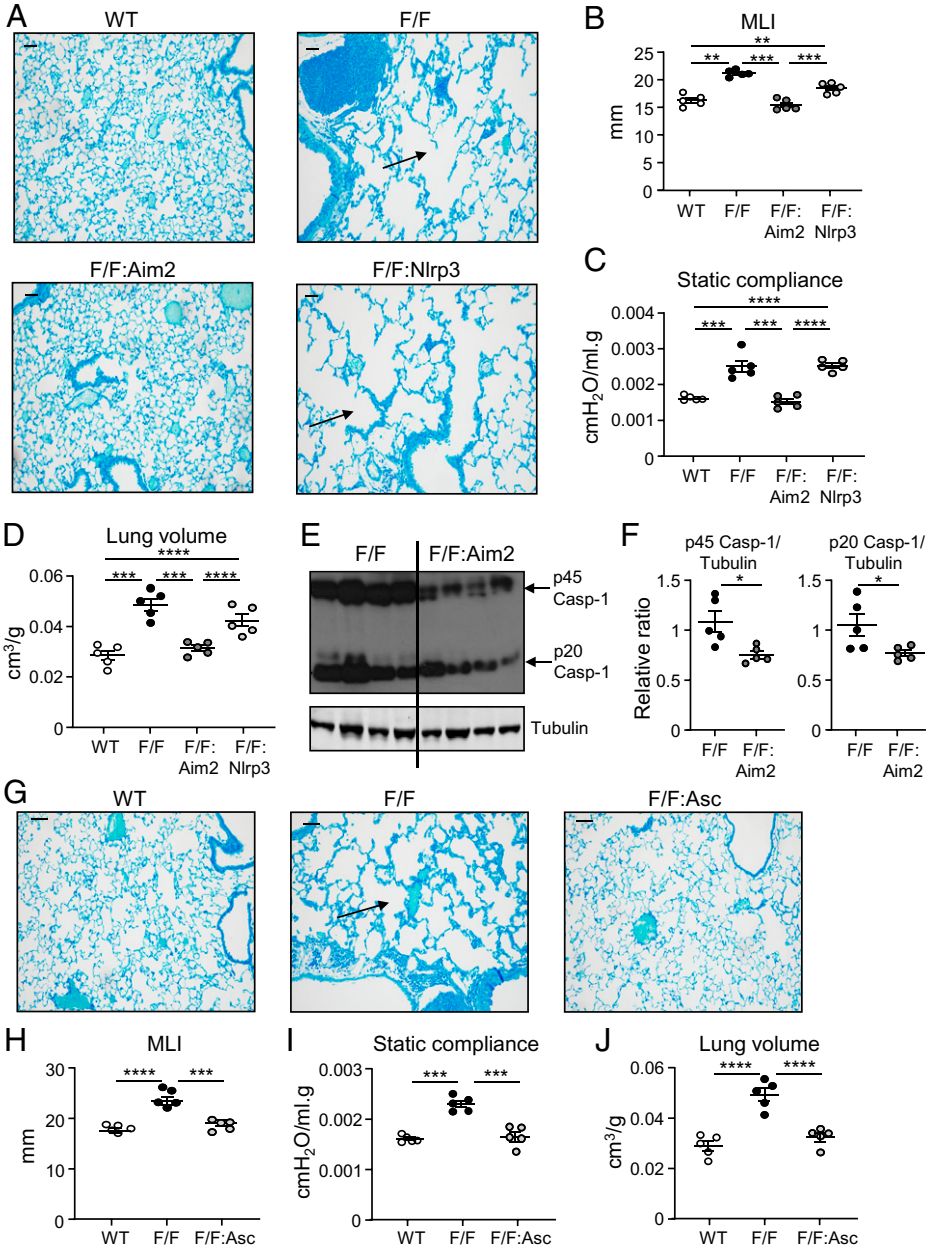

Fig. 2. Genetic ablation of AIM2 and ASC, but not NLRP3, suppresses emphysema in *gp130*$^{F/F}$ mice. (*A*) Representative methylene blue-stained cross-sections of lungs from 6mo WT, *gp130*$^{F/F}$ (F/F), *gp130*$^{F/F}$:*Aim2*$^{-/-}$ (F/F:Aim2), and *gp130*$^{F/F}$:*Nlrp3*$^{-/-}$ (F/F:Nlrp3) mice. Arrows point to representative areas of airspace enlargement. (Scale bars, 100 μm.) (*B–D*) Graphs depict (*B*) MLI, (*C*) static compliance, and (*D*) lung volume/body weight (grams) of indicated 6mo mice. $n = 5$ per genotype. $^{**}P < 0.01$, $^{***}P < 0.001$, $^{****}P < 0.0001$; one-way ANOVA. (*E*) Representative immunoblots on lung lysates from 6mo F/F and F/F:Aim2 mice for pro (45 kDa) and cleaved/mature (20 kDa) Caspase-1. (*F*) Densitometric quantification of immunoblots for pro and mature Caspase-1, normalized against tubulin. $n = 5$ per genotype. $^{*}P < 0.05$; Student's *t* test. (*G*) Representative methylene blue-stained cross-sections of lungs from 6mo WT, F/F, and *gp130*$^{F/F}$:*Asc*$^{-/-}$ (F/F:Asc) mice. Arrow points to a representative area of airspace enlargement. (Scale bars, 100 μm.) (*H–J*) Graphs depict (*H*) MLI, (*I*) static compliance, and (*J*) lung volume/body weight (grams) of indicated 6mo mice. $n = 5$ per genotype. $^{***}P < 0.001$, $^{****}P < 0.0001$; one-way ANOVA.

inflammasome)-mediated apoptosis, protein expression levels of full-length GSDMD were comparable among lung lysates of 6mo WT, *gp130*$^{F/F}$, and *gp130*$^{F/F}$:*Aim2*$^{-/-}$ mice, with no detectable levels of the mature N-terminal GSDMD p30 fragment (*SI Appendix*, Fig. S6*C*). Collectively, these data suggest that the AIM2 inflammasome promotes ATII cells to undergo apoptosis during emphysema.

Therapeutic Blockade of AIM2 Prevents Alveolar Cell Death and Emphysema in *gp130*$^{F/F}$ Mice. Immunosuppressive oligodeoxynucleotides (Sup ODN) exhibit potent antagonistic activity against AIM2 (26, 31). To determine whether AIM2 can serve as a bona fide therapeutic target in emphysema, we explored whether Sup ODN-mediated blockade of AIM2 activation would prevent emphysema development in *gp130*$^{F/F}$ mice from 3 months of age onward. At the completion of 10-wk treatment with Sup ODN, static compliance and lung volume of Sup ODN-treated *gp130*$^{F/F}$ mice were significantly reduced compared to control ODN (Ctl)-treated *gp130*$^{F/F}$ mice (*SI Appendix*, Fig. S7 *A* and *B*). Also, the number of ATII apoptotic cells was significantly reduced in the lungs of Sup ODN-treated *gp130*$^{F/F}$ mice (*SI Appendix*, Fig. S7 *C–F*). Collectively, these data demonstrate that therapeutic targeting of AIM2 activation can prevent emphysema development in *gp130*$^{F/F}$ mice.

Targeting AIM2 in an Acute CS Exposure Model of Emphysema Suppresses CS-Induced Alveolar Cell Apoptosis. We next assessed whether the AIM2 inflammasome also drives ATII cellular apoptosis that is a hallmark of an acute CS exposure model of emphysema (7, 8). Upon 4-d CS exposure of 6-wk-old WT mice, *Aim2* (but not *Nlrp3*) and *Pycard* mRNA levels were significantly increased compared to non-CS-exposed control mice, with immunofluorescence indicating colocalization of AIM2 (nuclear and cytoplasmic) with SPC-positive ATII cells and CD45-positive immune cells (Fig. 4*D* and *SI Appendix*, Fig. S8*A*). Acute CS exposure also significantly augmented pro and active Caspase-1 and pro and mature IL-1β levels (Fig. 4 *D–G* and *SI Appendix*, Fig. S8 *B* and *C*). Interestingly, staining of AIM2 colocalized with gamma-H2AX, a biomarker for double-stranded DNA damage, consistent with

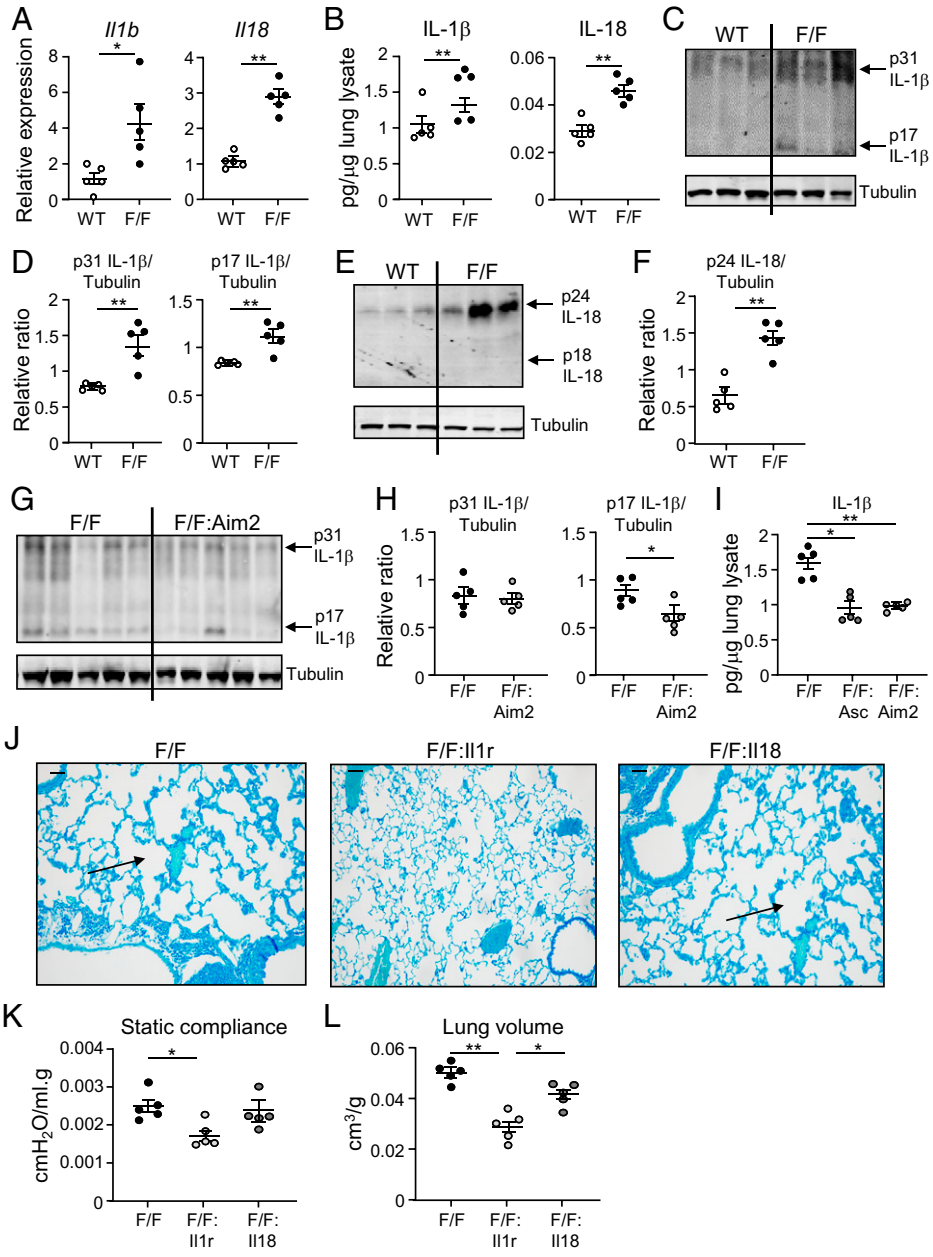

Fig. 3. Up-regulated production of IL-1β, but not IL-18, is associated with emphysema in *gp130*$^{F/F}$ mice. (*A*) qPCR on lung tissue of 6mo WT and *gp130*$^{F/F}$ (F/F) mice. Expression data normalized for 18S rRNA. $n = 5$ per genotype. *$P < 0.05$, **$P < 0.01$; Student's *t* test. (*B*) IL-1β and IL-18 ELISA on lung tissue lysates of 6mo WT and F/F mice. $n = 5$ per genotype. **$P < 0.01$; Student's *t* test. (*C* and *E*) Immunoblotting for (*C*) pro (31 kDa) and mature (17 kDa) IL-1β and (*E*) pro (24 kDa) and mature (18 kDa) IL-18 in lung lysates from indicated 6mo genotypes. (*D* and *F*) Densitometric quantification of immunoblots for pro and mature (*D*) IL-1β and (*F*) IL-18, normalized against tubulin. $n = 5$ per genotype. **$P < 0.01$; Student's *t* test. (*G*) Immunoblotting for pro and mature IL-1β in lung lysates from indicated 6mo genotypes. (*H*) Densitometric quantification of immunoblots (from *G*) for pro and mature IL-1β, normalized against tubulin. $n = 5$ per genotype. *$P < 0.05$; Student's *t* test. (*I*) IL-1β ELISA on lung tissue lysates from indicated 6mo mouse genotypes. $n = 5$ per genotype. *$P < 0.05$, **$P < 0.01$; one-way ANOVA. (*J*) Representative methylene blue-stained cross-sections of lungs from 6mo F/F, *gp130*$^{F/F}$:*Il1r*$^{-/-}$ (F/F:Il1r), and *gp130*$^{F/F}$:*Il18*$^{-/-}$ (F/F:Il18) mice. Arrow points to representative areas of airspace enlargement. (Scale bars, 100 μm.) (*K* and *L*) Graphs depict (*K*) static compliance and (*L*) lung volume/body weight (grams) of indicated 6mo mice. $n = 5$ per genotype. *$P < 0.05$, **$P < 0.01$; one-way ANOVA.

AIM2 being activated by damaged DNA that is a feature of CS exposure (32, 33) (*SI Appendix*, Fig. S8*D*). Moreover, while acute CS exposure of WT mice increased numbers of TUNEL-positive apoptotic alveolar cells, no such increases were observed in either CS-exposed *Aim2*$^{-/-}$ mice or CS-exposed WT mice treated with Sup ODN (Fig. 4 *H* and *I*). By contrast, in the lungs of *Nlrp3*$^{-/-}$ mice, NLRP3 deficiency had no effect on ameliorating CS-induced alveolar cell apoptosis (Fig. 4 *J* and *K*). These data therefore confirm that AIM2 drives alveolar cell apoptosis that is a hallmark of CS-induced emphysema.

Up-Regulation of AIM2 Inflammasome Components in Human Emphysema. We next assessed the expression of AIM2 and inflammasome-related genes in human lung tissues from patients with emphysema, defined by pulmonary lung function tests (gas exchange, FEV1) (*SI Appendix*, Table S1), as well as emphysema-free individuals. Among inflammasome-associated PRRs, only mRNA levels for *AIM2* were significantly up-regulated in lungs of emphysema patients compared with emphysema-free individuals (Fig. 5*A*). In addition, *PYCARD* and *CASP1* gene expression was significantly higher in emphysema patients, with expression of *PYCARD* significantly correlating with that of

AIM2 in emphysematous patient lungs (Fig. 5 *B* and *C*). Immunohistochemistry also demonstrated a significant increase in the number of AIM2- and active (p20) Caspase-1–positive cells in lung sections of emphysema patients, which was associated with a significant positive correlation in AIM2 and active Caspase-1 cellular staining in human lungs (Fig. 5 *D*–*H*). Notably, we also observed a significant increase in the number of AIM2- and active Caspase-1–positive cells in the lungs of smokers (current and former) compared to never smokers (Fig. 5 *D* and *F*). With respect to the inflammasome effector cytokines IL-1β and IL-18, mRNA levels for *IL1B* were elevated by ∼3-fold in emphysematous human lung tissues, with IL-1β protein levels elevated by ∼15- and ∼7-fold in lung and sera, respectively, of emphysema patients compared to emphysema-free individuals (Fig. 5 *I* and *J*). By contrast, *IL18* mRNA levels were comparable between emphysema patients and emphysema-free controls, and an ELISA specific for the mature form of human IL-18 also demonstrated comparable tissue levels in the lungs of emphysema and emphysema-free individuals (Fig. 5 *I* and *K*). Total IL-18 protein levels were below the level of detection by sandwich ELISA in emphysema patient lung tissue and sera. Overall, these clinical data are consistent with our in vivo findings and provide translational evidence for a pathologic role for the AIM2 inflammasome/IL-1β axis in human emphysema.

Up-Regulation of the AIM2 Inflammasome/IL-1β Axis in Pulmonary Emphysema Is Downstream of IL-6. Our finding that among inflammasome-associated PRRs only AIM2 is up-regulated in emphysematous lungs raises the question as to the upstream mechanism(s) by which AIM2 expression is induced during emphysema. In this respect, the capacity of AIM2 to promote alveolar cell apoptosis is strikingly reminiscent of the emphysema-causing functions of the cytokine, IL-6, which upon its up-regulation in the lung engages with the soluble IL-6R to elicit its proapoptotic trans-signaling mode (7, 8). In the lungs of emphysema-free $gp130^{F/F}$:$Aim2^{-/-}$ mice, since IL-6 expression levels (mRNA and protein) remain elevated compared to $gp130^{F/F}$ mice (*SI Appendix*, Fig. S4 *C* and *D*), we explored whether up-regulated expression of AIM2, and subsequent inflammasome activation, may be modulated upstream by IL-6. Indeed, *Aim2*, but not *Nlrp3*, mRNA levels were significantly lower in the lungs of emphysema-free $gp130^{F/F}$:$Il6^{-/-}$ mice (7, 8) compared to $gp130^{F/F}$ mice at early onset (3 mo) or established (6 mo) stages of emphysema (Fig. 6*A*). We note that pulmonary inflammation in $gp130^{F/F}$ mice is more pronounced at 6 mo versus 3 mo of age (8), yet the increased *Aim2* expression in the lungs of $gp130^{F/F}$ mice is comparable (∼3.5-fold) between these ages, suggesting that elevated *Aim2* mRNA levels are not a consequence of chronic immune/inflammatory cell infiltrates. These observations in $gp130^{F/F}$ mice were confirmed upon blockade of IL-6 trans-signaling by crossing $gp130^{F/F}$ mice with transgenic $sgp130Fc^{tg/tg}$ mice overexpressing the specific IL-6 trans-signaling antagonist sgp130Fc (34, 35), which resulted in significantly lower mRNA levels for *Aim2*, but not *Nlrp3*, in the lungs of $gp130^{F/F}$:$sgp130Fc^{tg/tg}$ versus $gp130^{F/F}$ mice (Fig. 6*B*). Similarly, upon acute CS exposure to either $sgp130Fc^{tg/tg}$ mice or WT mice treated with recombinant sgp130Fc, which in both cases suppresses augmented alveolar cell death (7), blockade of IL-6 trans-signaling significantly suppressed expression of *Aim2*, but not *Nlrp3*, compared to CS-exposed WT mice treated with vehicle (Fig. 6*C*). Immunohistochemistry also confirmed significantly reduced numbers of AIM2-positive cells throughout the lung parenchyma of $gp130^{F/F}$:$Il6^{-/-}$ versus $gp130^{F/F}$ mice (Fig. 6 *D* and *E*). Furthermore, expression levels of mature (and pro) Caspase-1 and IL-1β were markedly lower in lungs of $gp130^{F/F}$:$Il6^{-/-}$ versus $gp130^{F/F}$ mice (Fig. 6 *F*–*I*), consistent with reduced inflammasome activity in the absence of IL-6. In support of these in vivo observations, in a clinical setting we observed a significant positive correlation between IL-1β and IL-6, and IL-1β and sIL-6R, protein levels in the sera of emphysema patients (Fig. 6*J*). Collectively, these data suggest that the AIM2 inflammasome/IL-1β axis is up-regulated downstream of IL-6 during emphysema.

Discussion

The last decade has seen an increasing awareness of the critical role that innate (and adaptive) immune responses play in driving chronic pulmonary inflammation, one of the hallmarks of COPD. For instance, the constant exposure of airway and alveolar epithelial cells to inhaled infectious agents and/or noxious particulate matter, especially CS, can lead to the sustained production of a myriad of innate immune inflammatory cytokines (e.g., IL-1β, IL-6, and tumor necrosis factor α) and chemokines that promote the recruitment and activation of inflammatory cells (e.g., macrophages and neutrophils) into the lungs (3, 7, 8). In COPD, the chronic activation of these immune/inflammatory cells leads to the amplified release of inflammatory mediators, as well as DNA-damaging reactive oxygen species and tissue-destructive proteases, which collectively trigger excessive alveolar epithelial cell apoptosis and the progressive destruction of lung parenchyma (i.e., emphysema) (3). Despite these observations, the molecular regulators of innate immunity that orchestrate these pathological cellular processes leading to emphysema remain ill-defined.

Here, we reveal a hitherto unknown role for the innate immune AIM2 DNA sensor in driving emphysema that is independent of its expression in hematopoietic-derived immune cells and effect on infiltrating immune cells but rather involves inflammasome-mediated apoptosis of the alveolar epithelium. Indeed, the spontaneous onset of alveolar cell apoptosis and emphysema in the preclinical $gp130^{F/F}$ model was similarly abrogated in both $gp130^{F/F}$:$Asc^{-/-}$ and $gp130^{F/F}$:$Aim2^{-/-}$ mice and characterized by a marked reduction in the activation of Caspase-1. Among inflammasome-associated PRRs, AIM2 was the most highly up-regulated in the lungs of emphysematous $gp130^{F/F}$ mice, WT mice exposed to acute CS-induced alveolar cell apoptosis, and emphysematous patients and smokers, suggesting that AIM2 is the predominant inflammasome-associated PRR implicated in the pathogenesis of emphysema. Indeed, this notion is also supported by our findings that NLRP3 deficiency in $gp130^{F/F}$ mice did not protect against emphysema or reduce the activation of Caspase-1 in the lung, and $Nlrp3^{-/-}$ mice were not protected against CS-induced alveolar cell apoptosis. Importantly, our clinical data for AIM2 in emphysematous patients is supported by a recent report showing that in an independent small COPD patient cohort AIM2 is up-regulated in the airway epithelium and associates with GOLD disease stage (36). Although the mechanistic basis by which AIM2 is up-regulated in COPD was not reported, our current study demonstrates that increased pulmonary expression of AIM2 in emphysema was dependent on the upstream cytokine IL-6 and its trans-signaling axis (involving sIL-6R) which can be selectively blocked with the sgp130Fc antagonist.

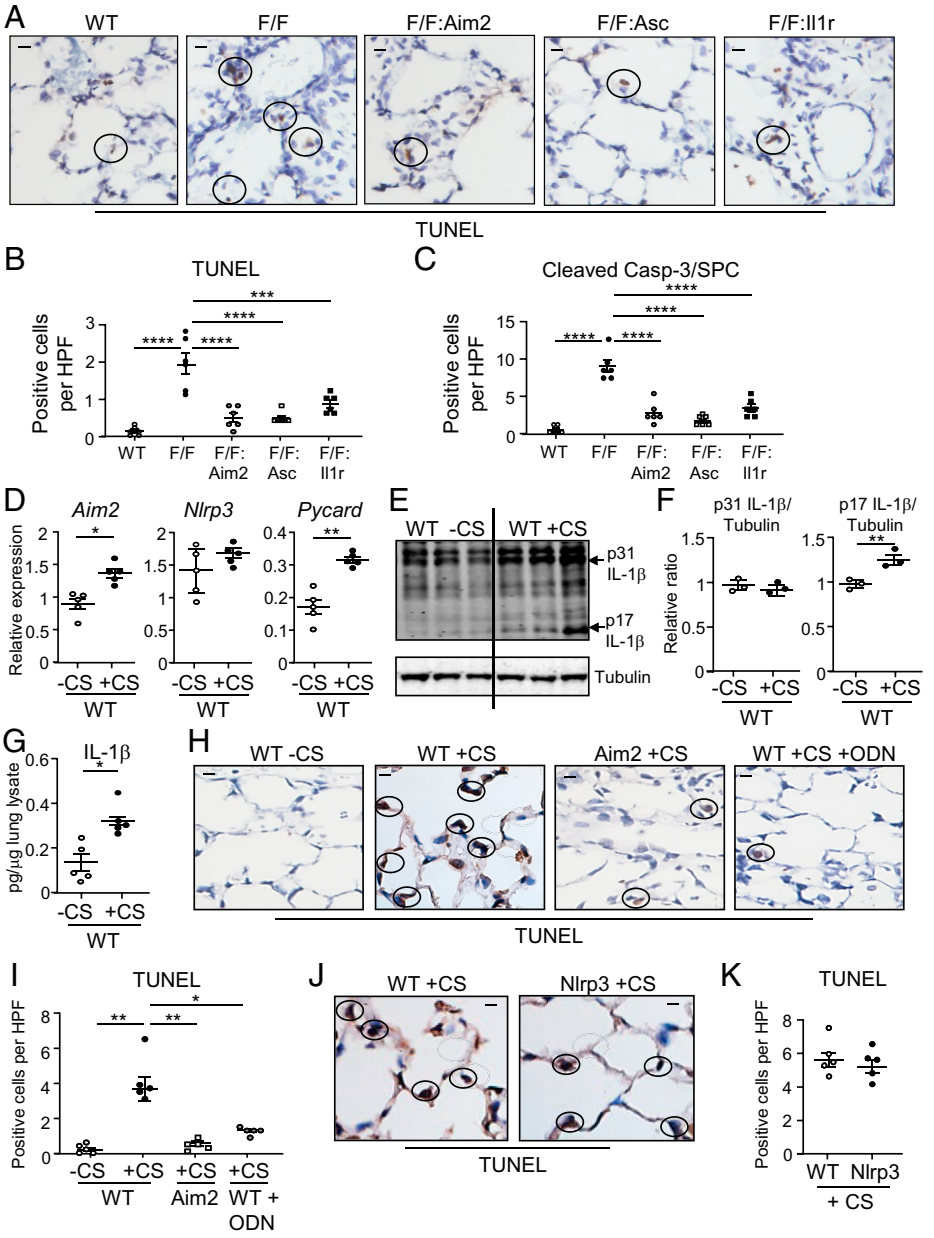

Fig. 4. AIM2 inflammasome-driven emphysema in the *gp130*$^{F/F}$ and CS models is associated with augmented apoptosis of alveolar type II epithelial cells. (*A*) Representative photomicrographs of cross-sections of lungs from 6mo WT, *gp130*$^{F/F}$ (F/F), *gp130*$^{F/F}$:*Aim2*$^{-/-}$ (F/F:Aim2), *gp130*$^{F/F}$:*Asc*$^{-/-}$ (F/F:Asc), and *gp130*$^{F/F}$:*Il1r*$^{-/-}$ (F/F:Il1r) mice subjected to TUNEL assay. Representative TUNEL-positive apoptotic lung cells are circled. (Scale bars, 25 μm.) (*B* and *C*) Graphs depict quantification of numbers of apoptotic (*B*) TUNEL-positive cells and (*C*) dual-labeled cleaved Caspase-3/SPC–positive alveolar type II epithelial cells per high-power field (HPF) in lungs of indicated 6mo mice. $n = 6$ per genotype. ***$P < 0.001$, ****$P < 0.0001$; one-way ANOVA. (*D*) qPCR (normalized for 18S rRNA) on lung tissue from WT mice exposed to acute CS (+CS) or sham air (−CS). $n = 5$ per group. *$P < 0.05$, **$P < 0.01$; Student's *t* test. (*E*) Immunoblots on lung lysates from indicated groups from *A* for pro (31 kDa) and mature (17 kDa) IL-1β. (*F*) Densitometric quantification of immunoblots from *E* for pro and mature IL-1β, normalized against tubulin. $n = 3$ per group. **$P < 0.01$; Student's *t* test. (*G*) IL-1β ELISA on lung tissue lysates from indicated groups. $n = 5$ per group. *$P < 0.05$; Student's *t* test. (*H* and *J*) Representative photomicrographs of TUNEL-stained cross-sections of lungs from (*H*) WT mice +CS or −CS, the former also treated with Sup ODN (15 mg/kg), or *Aim2*$^{-/-}$ mice (Aim2) +CS and (*J*) WT and *Nlrp3*$^{-/-}$ mice (Nlrp3) +CS, for 4 d. Representative TUNEL-positive apoptotic lung cells are circled. (Scale bars, 25 μm.) (*I* and *K*) Quantification of apoptotic TUNEL-positive cell numbers in lungs from mouse groups in (*I*) *H* and (*K*) *J*. $n = 5$ per group. *$P < 0.05$, **$P < 0.01$; one-way ANOVA.

AIM2 was recently shown to be transcriptionally up-regulated in gastric cancer via activation of the latent transcription factor STAT3 induced by IL-11, a member of the IL-6 cytokine family (26). While this suggests that IL-6 trans-signaling may also activate STAT3 in the lung to up-regulate AIM2 and promote emphysema, we note that STAT3 is not employed by IL-6 to promote alveolar cell apoptosis in emphysema (37). It will therefore be of most interest to further delineate the molecular pathways downstream of IL-6 trans-signaling that modulate AIM2 expression in the lung, such as mTOR, which is implicated in IL-6-driven emphysema (7). In addition, our current findings also warrant investigations on larger emphysematous COPD patient cohorts for the coexistence of up-regulated AIM2 inflammasome and IL-6 trans-signaling components and their clinical utility as markers of disease activity and targets for potential therapy.

In light of our finding that the AIM2 inflammasome in the lung augments alveolar cell apoptosis in emphysema, we note that the AIM2 inflammasome can induce both pyroptotic and apoptotic cell death via activation of Caspase-1 and -3, respectively, with low concentrations of AIM2-activating DNA agonists

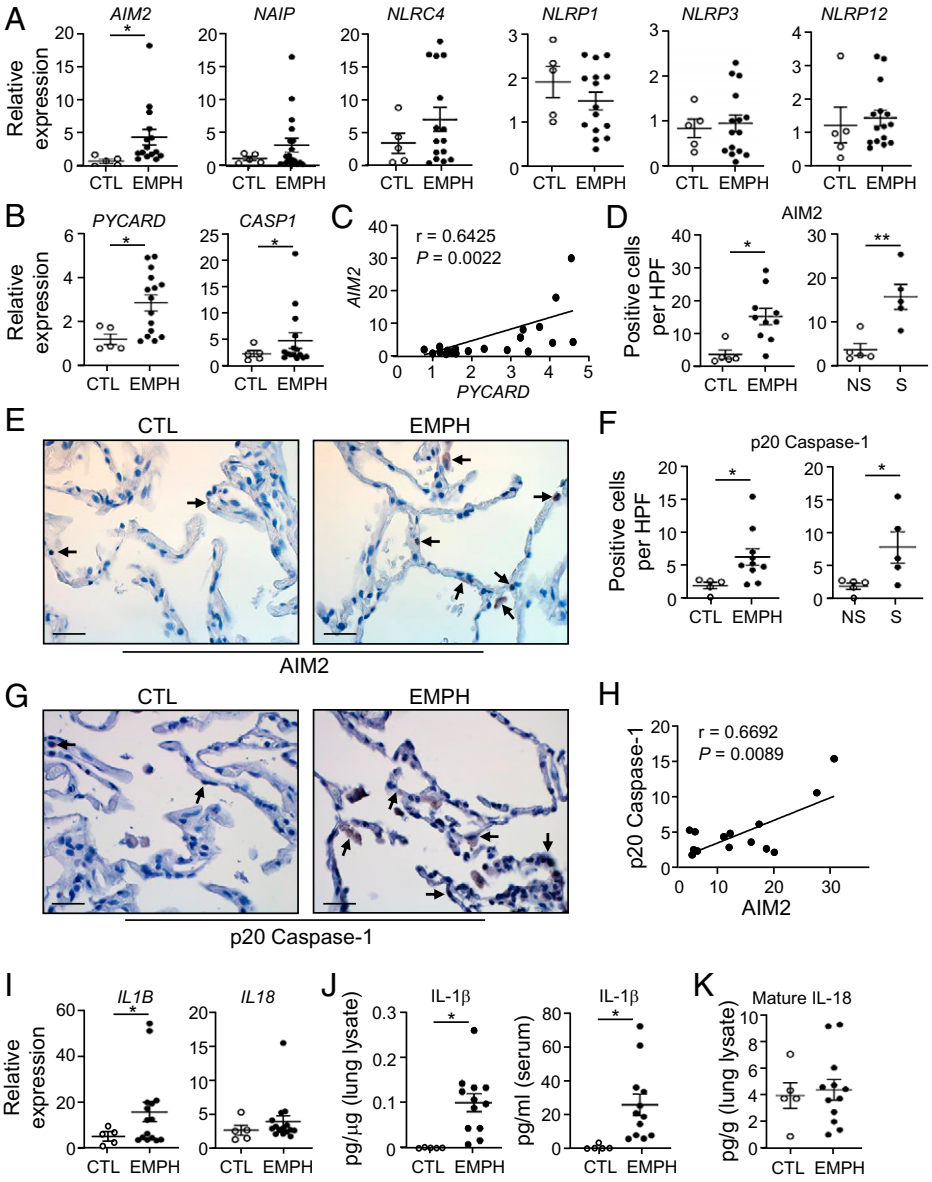

Fig. 5. Augmented expression and activation of AIM2 inflammasome components in emphysema patient lung tissues and sera. (*A* and *B*) qPCR on lungs of emphysema patients (EMPH, $n = 15$) or emphysema-free control individuals (CTL, $n = 5$). Expression data normalized for 18S rRNA. $^*P < 0.05$; Student's *t* test. (*C*) Correlation analyses of *AIM2* and *PYCARD* gene expression in lungs of emphysema patients ($n = 20$). r, Pearson correlation coefficient. (*D* and *F*) Graphs depicting quantification of (*D*) AIM2- and (*F*) cleaved Caspase-1–positive staining cell numbers per high-power field (HPF) in lungs of emphysema patients ($n = 10$) or emphysema-free control individuals ($n = 5$), plus individuals stratified as nonsmokers (NS; $n = 5$) or current smokers (S; $n = 5$). $^*P < 0.05$, $^{**}P < 0.01$; Student's *t* test. (*E* and *G*) Representative photomicrographs of lung cross-sections from emphysema patients or emphysema-free controls stained for human (*E*) AIM2 or (*G*) cleaved Caspase-1. Arrows depict representative positively stained cells. (Scale bars, 20 μm.) (*H*) Correlation analyses of immunohistochemical staining between AIM2 and cleaved Caspase-1 in lung sections from emphysema patients and emphysema-free controls ($n = 14$). r, Pearson correlation coefficient. (*I*) qPCR (normalized for 18S rRNA) on lungs of emphysema patients or emphysema-free controls from *A* and *B*. $^*P < 0.05$; Student's *t* test. (*J* and *K*) ELISA for (*J*) total IL-1β and (*K*) mature IL-18 in emphysema patients ($n = 12$) or emphysema-free controls ($n = 5$). $^*P < 0.05$; Mann–Whitney *U* test.

favoring apoptosis over pyroptosis (38, 39). Our current findings indicate that AIM2-driven cell death in the alveolar epithelium is associated with elevated levels of apoptotic Caspase-3–positive cells, which is reminiscent of the role assigned to AIM2, albeit in an inflammasome-independent manner, in the intestinal epithelium to promote Caspase-3–associated apoptosis during intestinal carcinogenesis (40). As a sensor of DNA damage, the AIM2 inflammasome has also been shown to promote cell death in intestinal epithelial cells following radiation-induced nuclear DNA damage (41). Together with the knowledge that CS exposure triggers double-strand DNA damage and cell death in lung epithelial cells (32, 42), and our current data demonstrating that AIM2 is both up-regulated by CS and colocalizes with cellular DNA damage in the alveolar epithelium during emphysema, we propose that the levels of cellular DNA damage in the lung detected by AIM2, leading to its inflammasome activation, occur at a threshold favoring Caspase-3–related apoptosis over Caspase-1–mediated pyroptosis. In this respect, we also show here that expression levels of GSDMD, which is required for pyroptotic, but not apoptotic, cell death triggered by Caspase-1 (i.e., inflammasomes) (43–45), were unchanged among the lungs of mice irrespective of Caspase-1 activation levels, as well as the absence or presence of emphysema. Interestingly, Caspase-1 has been shown to promote apoptosis in a Caspase-3–dependent manner in certain cell types harboring low GSDMD expression levels (44), suggesting that GSDMD

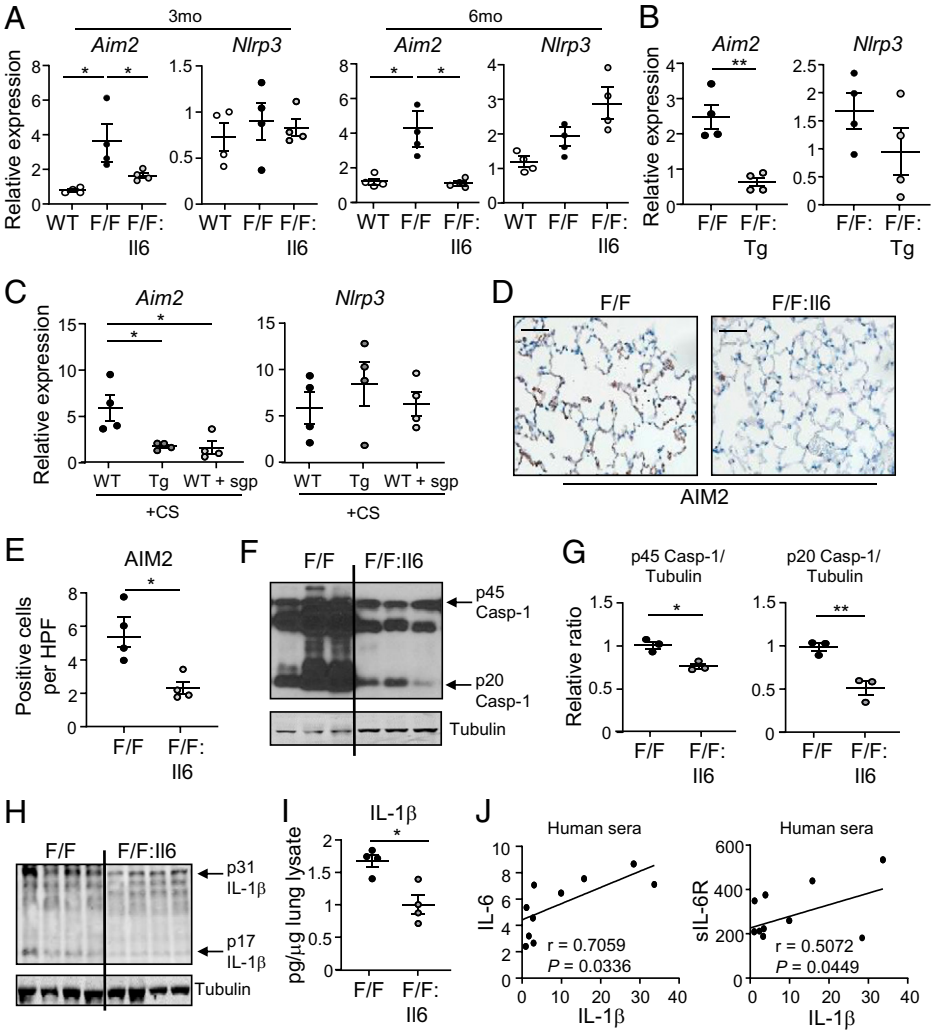

Fig. 6. AIM2 expression and inflammasome activation are up-regulated by IL-6 trans-signaling in emphysematous lungs. (*A–C*) qPCR (normalized for 18S rRNA) on lung tissue from (*A*) 3-month-old (mo) and 6mo WT, *gp130*$^{F/F}$ (F/F), and *gp130*$^{F/F}$:*Il6*$^{-/-}$ (F/F:Il6) mice, (*B*) F/F and *gp130*$^{F/F}$:*sgp130Fc*$^{tg/tg}$ (F/F:Tg) mice, and (*C*) WT mice, *sgp130Fc*$^{tg/tg}$ (Tg) mice and WT mice treated with sgp130Fc (WT+sgp), exposed to CS (+CS) for 4 d. $n = 4$ mice per group. *$P < 0.05$, **$P < 0.01$; (*A* and *C*) one-way ANOVA and (*B*) Student's *t* test. (*D*) Representative photomicrographs of AIM2-stained cross-sections of lungs from F/F and F/F:Il6 mice. (Scale bars, 100 μm.) (*E*) Quantification of AIM2-positive cells in cross-sections of lungs from indicated mouse genotypes. $n = 4$ per group. *$P < 0.05$; Student's *t* test. (*F*) Representative immunoblots on lung lysates from F/F and F/F:Il6 mice for pro (45 kDa) and cleaved (20 kDa) Caspase-1. (*G*) Densitometric quantification of immunoblots (in *F*) for protein levels of pro and cleaved Caspase-1, normalized against tubulin. $n = 3$ per group. *$P < 0.05$, **$P < 0.01$; Student's *t* test. (*H*) Representative immunoblots on lung lysates from F/F and F/F:Il6 mice for pro (31 kDa) and mature (17 kDa) IL-1β. (*I*) IL-1β ELISA on lung tissue lysates from indicated mice. $n = 4$ per group. *$P < 0.05$; Student's *t* test. (*J*) Correlation analyses of serum protein levels (ELISA) between IL-1β and either IL-6 or sIL-6R in emphysema patients ($n = 10$). r, Pearson correlation coefficient.

expression in the lung epithelium may be at sufficiently low levels to facilitate Caspase-1–mediated apoptosis (via Caspase-3) rather than pyroptosis. It will therefore be of most interest to further interrogate the relative contribution and interplay of additional cell death caspases (e.g., Caspase-7, -8, and -9) and pathways (e.g., Bcl-2 homology [BH]3-only proteins) employed by AIM2 to promote apoptosis in the lung during emphysema.

Our data suggesting that NLRP3 does not play a critical role in driving the onset of pulmonary inflammation and emphysema build on previous in vivo studies on COPD indicating that the lungs of *Nlrp3*$^{-/-}$ mice are largely unprotected against pulmonary inflammation induced by acute (3-d) or subacute (4-wk) whole-body exposure to CS (19, 23). Interestingly, NLRP3 deficiency led to a reduction in BALF neutrophils in response to acute CS exposure, whereas AIM2 deficiency had no impact on CS-up-regulation of BALF neutrophils, suggesting a specific role for NLRP3 in regulating CS-induced airway neutrophil infiltration (19). In another study in which *Nlrp3*$^{-/-}$ mice were subjected to CS inhalation over 12 mo, NLRP3 deficiency ameliorated airway obstruction and inflammatory responses (again only BALF was assessed) (25). However, unlike our current study, the role of NLRP3 in alveolar cellular apoptosis and airspace enlargement, which are hallmarks of emphysema, was not investigated in these CS-induced experimental COPD models. More recently, NLRP3 expression was shown to be up-regulated in an ozone-induced model of COPD characterized by pulmonary inflammation and alveolar airspace enlargement, and in which treatment with the Caspase-1 inhibitor VX-765 attenuated pulmonary inflammation and emphysema in WT ozone-administered mice (22). However, a causal role for NLRP3 in ozone-induced lung inflammation and emphysema was not investigated. Despite the unclear role of NLRP3 in driving CS-induced COPD-related lung pathologies, we note that the targeted blockade of NLRP3 with the pharmacological inhibitor MCC950 has been shown to ameliorate lung inflammation induced by bacterial lipopolysaccharide, suggesting that NLRP3 may contribute to COPD exacerbations related to infection (46).

Another finding of our current study was that the emphysema-promoting role of the AIM2 inflammasome was associated with the preferential processing and up-regulation of IL-1β but not IL-18. Although a role for IL-1β in contributing to the onset of emphysema has previously been suggested by the observation that *Il1r*$^{-/-}$ mice are markedly protected against emphysema following chronic (6-mo) exposure of CS (17), the identity of the upstream inflammasome-associated PRR involved has remained elusive; our current findings suggest AIM2 is the predominant inflammasome-associated PRR that processes IL-1β production during emphysema. In addition, a role for IL-18 in promoting emphysema has been reported, with the transgenic overexpression of IL-18 in the lungs of mice triggering emphysematous alveolar destruction and airspace enlargement, while mice lacking the IL-18 receptor subunit IL-18Rα are protected against chronic CS-induced emphysematous changes (including increased epithelial apoptosis) in the lung (18, 47). Interestingly, the role of both IL-1β and IL-18 in promoting CS-induced emphysema was coincident with elevated numbers in the lung of infiltrating immune cells, which differs from our current data that IL-1β, but not IL-18, promotes emphysema independent of changes in numbers of immune cell infiltrates in the lung. A likely explanation for these discrepancies lies in the different emphysema models used which encapsulate different molecular and cellular aspects of the complex pathogenesis of emphysema (e.g., apoptosis—as per our current study, inflammation, oxidative stress, protease activity). Indeed, future studies incorporating multicolor immunofluorescence are warranted to investigate whether the preferential availability of IL-1β by AIM2 inflammasomes for processing aligns with the cellular colocalization (e.g., ATII epithelial cells versus immune cells) of AIM2 inflammasome components (i.e., AIM2, Caspase-1, ASC) with IL-1β, and not IL-18, in the emphysematous lung. Furthermore, it is important to note that our current data for IL-1β in emphysema is in the context of a downstream effector for the AIM2 inflammasome, whereas in the aforementioned studies the upstream activators of IL-1β and IL-18 production are unknown and could involve mechanisms that are independent of the AIM2/ASC/Caspase-1 inflammasome complex.

We also refer our findings to previous studies investigating inflammasome-related components and effector cytokines in CS-induced airway inflammation, which along with emphysema is another key feature of COPD. Reduced numbers of neutrophils in BALF of *Il1b*$^{-/-}$ (and *Il18*$^{-/-}$) mice in response to acute CS challenge have been reported (19), and mice treated with an anti–IL-1β antibody are significantly protected against CS-induced increases in total BALF inflammatory cells (23). While these findings support a role for IL-1β in CS-induced inflammatory responses in the lung, there was no disease association between IL-1β and the NLRP3/Caspase-1 axis, since neither *Casp1*$^{-/-}$ nor *Nlrp3*$^{-/-}$ mice were protected against CS-induced increases in immune cells in BALF (23). In this respect, our current study also questions the importance of inflammasome-mediated processing of IL-1β for pulmonary inflammation, since lung immune cell infiltrates were not attenuated in emphysema-free *gp130*$^{F/F}$ mice lacking either ASC, AIM2, or IL-1R, despite ASC or AIM2 deficiency resulting in reduced IL-1β protein levels. We also note a recent study using an AIM2 gene-trap mouse strain that curiously displayed increased airway inflammation and alveolar diameter at baseline (i.e., air exposure) compared to WT controls, yet upon 10-wk CS exposure increases in alveolar diameter and tissue destruction were comparable to CS-exposed WT mice (48). These findings that contrast with our current study are likely explained by key differences in study design, including genetic background of mice and duration of CS exposure (i.e., 4 d versus 10 wk), the latter of which may suggest that AIM2 plays contrasting roles in acute versus chronic CS exposure. We also note that AIM2 gene-trap mice display residual AIM2 expression and can sensitize the immune system toward hyperinflammatory responses (49), which might confound interpretation of the effect of AIM2 deficiency on lung-based parameters upon CS exposure (versus WT mice).

In conclusion, our study demonstrates a specific pathological role for the AIM2 inflammasome in emphysema, in which we delineate a function for AIM2 in modulating alveolar cell apoptosis that is independent of immune cell activity and inflammatory responses. In emphysematous lungs, AIM2, but not NLRP3, acts as the primary inflammasome-associated PRR that regulates Caspase-1 activation and processing of IL-1β. While our current study is based on stable COPD/emphysema, it will be of interest for future studies to also investigate the role of AIM2 during recurrent infection and serious exacerbations of COPD, which accelerate lung function decline in patients. We also note that, to date, the therapeutic targeting of IL-1β in COPD, for instance with neutralizing monoclonal antibodies against either IL-1β (Canakinumab) or IL-1R1 (MEDI8968) (50, 51), has not shown clinical efficacy. Since blocking IL-1β may also interfere with homeostatic immune responses that protect against opportunistic infections, our study paves the way to develop novel therapeutic approaches that block specific inflammasome components and associated distinct pathogenic processes of emphysema/COPD (i.e., AIM2-driven cellular apoptosis) without compromising the immune system.

Data, Materials, and Software Availability. All study data are included in the article and/or *SI Appendix*.

ACKNOWLEDGMENTS. We thank V. Hornung (Ludwig-Maximilians-Universität München) and K. Fitzgerald (University of Massachusetts Chan Medical School) for providing *Aim2*$^{-/-}$ and *Nlrp3*$^{-/-}$ mice, respectively. S.R.J. is supported by the Deutsche Forschungsgemeinschaft Bonn, Germany (SFB877, project A1 and the Cluster of Excellence "Precision Medicine in Inflammation"). This work was funded by a Project Grant (APP1139373) to B.J.J. from the National Health and Medical Research Council (NHMRC) and the Operational Infrastructure Support Program by the Victorian Government of Australia. B.J.J. was supported by an NHMRC Senior Research Fellowship.

Author affiliations: [a]Centre for Innate Immunity and Infectious Diseases, Hudson Institute of Medical Research, Clayton, VIC 3168, Australia; [b]Department of Molecular and Translational Science, Faculty of Medicine, Nursing and Health Sciences, Monash University, Clayton, VIC 3800, Australia; [c]Lung Health Research Centre, Department of Biochemistry and Pharmacology, The University of Melbourne, Parkville, VIC 3050, Australia; [d]Monash Lung and Sleep, Monash Health, Clayton, VIC 3168, Australia; [e]Division of Rheumatology, University Hospital of Geneva, H-1211 Geneva 14, Switzerland; [f]Department of Pathology and Immunology, University of Geneva School of Medicine, H-1211 Geneva 4, Switzerland; [g]Cancer and Inflammation Program, National Cancer Institute, Frederick, MD 21702; [h]School of Health and Biomedical Sciences, RMIT University, Bundoora, VIC 3083, Australia; and [i]Institute of Biochemistry, Christian Albrechts University, 24118 Kiel, Germany

1. K. F. Rabe, H. Watz, Chronic obstructive pulmonary disease. *Lancet* **389**, 1931–1940 (2017).
2. R. M. Tuder, I. Petrache, Pathogenesis of chronic obstructive pulmonary disease. *J. Clin. Invest.* **122**, 2749–2755 (2012).
3. G. G. Brusselle, G. F. Joos, K. R. Bracke, New insights into the immunology of chronic obstructive pulmonary disease. *Lancet* **378**, 1015–1026 (2011).
4. R. A. Pauwels, K. F. Rabe, Burden and clinical features of chronic obstructive pulmonary disease (COPD). *Lancet* **364**, 613–620 (2004).
5. G. C. Donaldson *et al.*, Airway and systemic inflammation and decline in lung function in patients with COPD. *Chest* **128**, 1995–2004 (2005).
6. J. Q. He *et al.*, Associations of IL6 polymorphisms with lung function decline and COPD. *Thorax* **64**, 698–704 (2009).

7. S. M. Ruwanpura *et al.*, Therapeutic targeting of the IL-6 trans-signaling/mechanistic target of rapamycin complex 1 axis in pulmonary emphysema. *Am. J. Respir. Crit. Care Med.* **194**, 1494–1505 (2016).
8. S. M. Ruwanpura *et al.*, Interleukin-6 promotes pulmonary emphysema associated with apoptosis in mice. *Am. J. Respir. Cell Mol. Biol.* **45**, 720–730 (2011).
9. C. Kuhn, 3rd *et al.*, Airway hyperresponsiveness and airway obstruction in transgenic mice. Morphologic correlates in mice overexpressing interleukin (IL)-11 and IL-6 in the lung. *Am. J. Respir. Cell Mol. Biol.* **22**, 289–295 (2000).
10. N. S. Pauwels *et al.*, The role of interleukin-6 in pulmonary and systemic manifestations in a murine model of chronic obstructive pulmonary disease. *Exp. Lung Res.* **36**, 469–483 (2010).
11. C. Garbers, S. Heink, T. Korn, S. Rose-John, Interleukin-6: Designing specific therapeutics for a complex cytokine. *Nat. Rev. Drug Discov.* **17**, 395–412 (2018).
12. X. Cao, Self-regulation and cross-regulation of pattern-recognition receptor signalling in health and disease. *Nat. Rev. Immunol.* **16**, 35–50 (2016).
13. G. dos Santos, M. A. Kutuzov, K. M. Ridge, The inflammasome in lung diseases. *Am. J. Physiol. Lung Cell. Mol. Physiol.* **303**, L627–L633 (2012).
14. M. G. Netea, F. L. van de Veerdonk, J. W. van der Meer, C. A. Dinarello, L. A. Joosten, Inflammasome-independent regulation of IL-1-family cytokines. *Annu. Rev. Immunol.* **33**, 49–77 (2015).
15. S. Tartey, T. D. Kanneganti, Inflammasomes in the pathophysiology of autoinflammatory syndromes. *J. Leukoc. Biol.* **107**, 379–391 (2020).
16. F. M. Botelho *et al.*, IL-1α/IL-1R1 expression in chronic obstructive pulmonary disease and mechanistic relevance to smoke-induced neutrophilia in mice. *PLoS One* **6**, e28457 (2011).
17. A. Churg, S. Zhou, X. Wang, R. Wang, J. L. Wright, The role of interleukin-1beta in murine cigarette smoke-induced emphysema and small airway remodeling. *Am. J. Respir. Cell Mol. Biol.* **40**, 482–490 (2009).
18. M. J. Kang *et al.*, IL-18 is induced and IL-18 receptor alpha plays a critical role in the pathogenesis of cigarette smoke-induced pulmonary emphysema and inflammation. *J. Immunol.* **178**, 1948–1959 (2007).
19. S. Eltom *et al.*, Role of the inflammasome-caspase1/11-IL-1/18 axis in cigarette smoke driven airway inflammation: An insight into the pathogenesis of COPD. *PLoS One* **9**, e112829 (2014).
20. S. Eltom *et al.*, P2X7 receptor and caspase 1 activation are central to airway inflammation observed after exposure to tobacco smoke. *PLoS One* **6**, e24097 (2011).
21. I. Couillin *et al.*, IL-1R1/MyD88 signaling is critical for elastase-induced lung inflammation and emphysema. *J. Immunol.* **183**, 8195–8202 (2009).
22. F. Li *et al.*, Roles of mitochondrial ROS and NLRP3 inflammasome in multiple ozone-induced lung inflammation and emphysema. *Respir. Res.* **19**, 230 (2018).
23. N. S. Pauwels *et al.*, Role of IL-1α and the Nlrp3/caspase-1/IL-1β axis in cigarette smoke-induced pulmonary inflammation and COPD. *Eur. Respir. J.* **38**, 1019–1028 (2011).
24. B. S. Franklin *et al.*, The adaptor ASC has extracellular and 'prionoid' activities that propagate inflammation. *Nat. Immunol.* **15**, 727–737 (2014).
25. W. Yang, H. Ni, H. Wang, H. Gu, NLRP3 inflammasome is essential for the development of chronic obstructive pulmonary disease. *Int. J. Clin. Exp. Pathol.* **8**, 13209–13216 (2015).
26. R. E. Dawson *et al.*, STAT3-mediated upregulation of the AIM2 DNA sensor links innate immunity with cell migration to promote epithelial tumourigenesis. *Gut* **71**, 1515–1531 (2022).
27. V. Deswaerte *et al.*, Inflammasome Adaptor ASC Suppresses Apoptosis of Gastric Cancer Cells by an IL18-Mediated Inflammation-Independent Mechanism. *Cancer Res.* **78**, 1293–1307 (2018).
28. T. D. Kanneganti *et al.*, Bacterial RNA and small antiviral compounds activate caspase-1 through cryopyrin/Nalp3. *Nature* **440**, 233–236 (2006).
29. C. Kilkenny, W. J. Browne, I. C. Cuthill, M. Emerson, D. G. Altman, Improving bioscience research reporting: The ARRIVE guidelines for reporting animal research. *PLoS Biol.* **8**, e1000412 (2010).
30. M. I. Saad *et al.*, ADAM17 selectively activates the IL-6 trans-signaling/ERK MAPK axis in KRAS-addicted lung cancer. *EMBO Mol. Med.* **11**, e9976 (2019).
31. J. J. Kaminski *et al.*, Synthetic oligodeoxynucleotides containing suppressive TTAGGG motifs inhibit AIM2 inflammasome activation. *J. Immunol.* **191**, 3876–3883 (2013).
32. S. S. Hecht, Tobacco carcinogens, their biomarkers and tobacco-induced cancer. *Nat. Rev. Cancer* **3**, 733–744 (2003).
33. L. J. Y. L. Kuo, L. X. Yang, Gamma-H2AX - a novel biomarker for DNA double-strand breaks. *In Vivo* **22**, 305–309 (2008).
34. B. Rabe *et al.*, Transgenic blockade of interleukin 6 transsignaling abrogates inflammation. *Blood* **111**, 1021–1028 (2008).
35. T. Jostock *et al.*, Soluble gp130 is the natural inhibitor of soluble interleukin-6 receptor transsignaling responses. *Eur. J. Biochem.* **268**, 160–167 (2001).
36. H. B. Tran *et al.*, AIM2 nuclear exit and inflammasome activation in chronic obstructive pulmonary disease and response to cigarette smoke. *J. Inflamm. (Lond.)* **18**, 19 (2021).
37. S. M. Ruwanpura *et al.*, Deregulated Stat3 signaling dissociates pulmonary inflammation from emphysema in gp130 mutant mice. *Am. J. Physiol. Lung Cell. Mol. Physiol.* **302**, L627–L639 (2012).
38. V. Sagulenko *et al.*, AIM2 and NLRP3 inflammasomes activate both apoptotic and pyroptotic death pathways via ASC. *Cell Death Differ.* **20**, 1149–1160 (2013).
39. T. Fernandes-Alnemri, J. W. Yu, P. Datta, J. Wu, E. S. Alnemri, AIM2 activates the inflammasome and cell death in response to cytoplasmic DNA. *Nature* **458**, 509–513 (2009).
40. S. M. Man *et al.*, Critical Role for the DNA Sensor AIM2 in Stem Cell Proliferation and Cancer. *Cell* **162**, 45–58 (2015).
41. B. Hu *et al.*, The DNA-sensing AIM2 inflammasome controls radiation-induced cell death and tissue injury. *Science* **354**, 765–768 (2016).
42. D. J. Slebos *et al.*, Mitochondrial localization and function of heme oxygenase-1 in cigarette smoke-induced cell death. *Am. J. Respir. Cell Mol. Biol.* **36**, 409–417 (2007).
43. P. Broz, P. Pelegrín, F. Shao, The gasdermins, a protein family executing cell death and inflammation. *Nat. Rev. Immunol.* **20**, 143–157 (2020).
44. K. Tsuchiya *et al.*, Caspase-1 initiates apoptosis in the absence of gasdermin D. *Nat. Commun.* **10**, 2091 (2019).
45. J. Shi *et al.*, Cleavage of GSDMD by inflammatory caspases determines pyroptotic cell death. *Nature* **526**, 660–665 (2015).
46. L. Wang, W. Lei, S. Zhang, L. Yao, MCC950, a NLRP3 inhibitor, ameliorates lipopolysaccharide-induced lung inflammation in mice. *Bioorg. Med. Chem.* **30**, 115954 (2021).
47. M. J. Kang *et al.*, IL-18 induces emphysema and airway and vascular remodeling via IFN-γ, IL-17A, and IL-13. *Am. J. Respir. Crit. Care Med.* **185**, 1205–1217 (2012).
48. C. Donovan *et al.*, Aim2 suppresses cigarette smoke-induced neutrophil recruitment, neutrophil caspase-1 activation and anti-Ly6G-mediated neutrophil depletion. *Immunol. Cell Biol.* **100**, 235–249 (2022).
49. M. El-Zaatari *et al.*, Aim2-mediated/IFN-β-independent regulation of gastric metaplastic lesions via CD8+ T cells. *JCI Insight* **5**, e94035 (2020).
50. P. Rogliani, L. Calzetta, J. Ora, M. G. Matera, Canakinumab for the treatment of chronic obstructive pulmonary disease. *Pulm. Pharmacol. Ther.* **31**, 15–27 (2015).
51. P. M. A. Calverley *et al.*, A randomised, placebo-controlled trial of anti-interleukin-1 receptor 1 monoclonal antibody MEDI8968 in chronic obstructive pulmonary disease. *Respir. Res.* **18**, 153 (2017).